Antithrombotic Effects of Montelukast by Targeting Coagulation Factor XIa

Dong Wang
Weifang Medical University
Yang Zhou
Fuzhou University
Yingying Qi
Fuzhou University
Meiru Song
Fuzhou University
Huiqiao Yao
Fuzhou University
Christopher Liao
Columbia University
Haili Lin
The Peoples Hospital of Fujian Province
Meijuan Huang
Fujian Medical University Union Hospital
Dexiang Zhuo
The Central Laboratory of Sanming First Hospital Affiliated to Fujian Medical University
Longguang Jiang
Fuzhou University
Cai Yuan
Fuzhou University
Yuanzhong Chen
Fujian Medical University
Mingdong Huang
Fuzhou University
Jinyu Li
Fuzhou University https://orcid.org/0000-0002-8220-049X
Peng Xu (pengxu@fzu.edu.cn)
Fuzhou University https://orcid.org/0000-0003-3968-7279

Article

Keywords: Coagulation factor XI, virtual screening, Montelukast, anticoagulants, thrombosis

Posted Date: May 10th, 2021

DOI: https://doi.org/10.21203/rs.3.rs-477725/v1

Abstract

Current oral anticoagulants prescribed for the prevention of thrombosis suffer from severe hemorrhagic problems. Coagulation factor XIa (FXIa) has been confirmed as a safer antithrombotic target as intervention with FXIa causes lower hemorrhagic risks. In this study, by a high-throughput virtual screening, we identified Montelukast (MK), an oral antiasthmatic drug, as a potent and specific FXIa inhibitor (IC_{50} = 0.17 μM). Compared with the two mostly prescribed anticoagulants (Warfarin and Apixaban), MK demonstrated comparable or even higher antithrombotic effects in three independent animal models. More importantly, in contrast to the severe hemorrhage caused by Warfarin or Apixaban, MK did not measurably increase blood loss *in vivo*. In addition, MK did not affect the hemostatic function in plasma from healthy individuals. In contrast, MK suppressed clot formation in clinical hypercoagulable plasma samples. This study provides a lead compound of anticoagulants targeting FXIa, and suggests the exploratory clinical researches on antithrombotic therapies using MK.

Introduction

Vascular fluidity is maintained by the equilibrium among platelet adhesion, coagulation, anticoagulation, and fibrinolysis[1]. Thrombosis (e.g. deep venous thrombosis, myocardial infarction, ischemic stroke, etc) is caused by the excessive activation of the coagulation system overwhelming the relatively insufficient anticoagulation and fibrinolytic systems leading to the obstruction in vessels by thrombi. Anticoagulants, intervening with the coagulation cascade and slow down fibrin deposition in vessels, are widely used for the preventions and treatments of venous thromboembolism (VTE) and for the prevention against coronary artery diseases (CADs) accompanied with antiplatelets. The most prescribed oral anticoagulants are vitamin-K-antagonists (VKAs) and the directly-acting-oral-anticoagulants (DOACs). VKAs reduce vitamin K activity required for the post-translational modification of coagulation factors [2]. DOACs are orally available inhibitors of coagulation factor Xa (FXa) or thrombin [3]. A common but significant adverse effect of these anticoagulants is the narrow therapeutic window: over-anticoagulation results in an inherently high risk of severe bleeding, while insufficient anticoagulation leads to thrombosis [4].

The ideal anticoagulant is considered to attenuate thrombosis while maintaining hemostatic functions. FX(a) and (pro)thrombin are simultaneously critical to thrombosis and hemostasis [5]. VKAs and DOACs directly or indirectly intervene with the activation, modification, or activity of (pro)thrombin and/or FX(a), thus impairing the hemostatic function and resulting in hemorrhage. Coagulation factor XI(a) (FXI/FXIa) was originally recognized to facilitate the generation of thrombin in the intrinsic cascade, a supplement of the tissue factor (TF)-triggered extrinsic cascade [6]. Clinically, patients with congenital FXI deficiency show no or mild hemorrhagic problems [7, 8]. Clinical evidences have confirmed that high levels of FXI in plasma are closely associated with thrombotic pathologies, including VTE [9], ischemic stroke [10], and myocardial infarction [11]. The role of FXI(a) in thrombosis can be complex. First, FXI, activated by thrombin or FXIIa, amplifies thrombin generation by sequentially activating FIX and FX [12]. Besides, in

CADs, rupture of an atherosclerotic plaque releases negatively charged substances activating FXII and FXI to enhance thrombin generation [13]. Furthermore, FXIa suppresses congenital anticoagulation by degrading tissue-factor-pathway-inhibitor (TFPI) [14], the physiological inhibitor of TF:FVIIa complex and FXIa. The above functions of FXI(a) are considered to be less relevant to hemostasis but crucial in thrombosis, because the amplification of thrombin generation enhances thrombi's resistance against fibrinolysis.

Thus, compared to (pro)thrombin or FX(a), FXI(a) is considered as a safer antithrombotic target to avoid severe hemorrhages. Intervention with FXI(a) has demonstrated promising outcomes in experimental models, pre-clinical studies, and clinical trials. An antisense oligonucleotide of FXI (FXI-ASO), which impairs the hepatic synthesis of FXI [15], has finished phase II clinical trial in Europe (ISIS-416858) [16]. FXI-ASO significantly reduced the incidences of VTE and VTE-related mortality with no observation of major bleeding [4]. BAY1213790, an IgG1 antibody that inhibits the activation of FXI, demonstrated favorable safety and tolerability in phase I clinical trial [17]. BMS-986177, an oral small-molecule FXIa inhibitor, is currently in phase II clinical trial of preventing post-surgical VTE events versus Enoxaparin (JNJ-70033093).

Although several molecules targeting FXI(a) are currently in clinical trials, only BMS-986177 is potentially orally available for the long-term prevention against thrombosis. However, the potential toxicities and side-effects have not been confirmed by the post-market surveillance. Thus, retargeting prescriptive drugs to FXI(a) is a strategy to achieve FXIa inhibitors with well-studied pharmacological properties and safeties. In this study, we identified Montelukast (MK), an FDA-approved antiasthmatic drug, as a potent FXIa inhibitor through a combination of *in silico* screening and experimental validation (IC_{50} = 0.17 μM). MK alleviates asthmatic symptoms by blocking cysteinyl leukotriene receptors (cys-LTRs) and thus suppressing smooth muscle contraction in the airway [18]. MK has been prescribed for the prevention of chronic asthmatic symptoms and for the relief of seasonal and perennial allergic rhinitis [19, 20]. Patients administered with MK generally demonstrate good tolerance, and only few of them showed mild side-effects [21]. MK has never been associated with coagulation or antithrombotic treatments, though subcutaneous bruising or mild nosebleed was observed as a rare side-effect, similar to the side-effect of anticoagulants, indicating that MK avoids impairing hemostatic functions.

The inhibitory potency of MK against FXIa, identified in this study, suggests its antithrombotic property. In addition, MK demonstrated specificity to FXIa showing non-measurable inhibition against homogenous proteases, especially thrombin and FXa, which are critical to hemostatic functions. Next, the molecular mechanisms of MK's inhibition and selectivity were revealed using molecular dynamics (MD) simulations. After confirming that MK inhibited FXIa-induced clot formation *in vitro*, we used three *in vivo* thrombotic models to evaluate MK's antithrombotic properties and compared with those of two clinically used anticoagulants, Warfarin (a VKA) and Apxaban (Apx, a DOAC). In addition, the hemorrhagic risks caused by MK, Warfarin, and Apx were evaluated and compared in a mouse tail bleeding model. We also

studied the influence of MK on the global coagulation in plasma from healthy individuals and clot formation in clinical hypercoagulable plasma samples.

Results

In silico screening

Based on the most representative structure of the catalytic domain of FXIa obtained from molecular dynamics (MD) simulations on its crystal structure (PDB ID: 4CRG [21]), we carried out a docking-based virtual screening against a customized drug repurposing library (3,727 compounds, Figure 1A) using Libdock and CDOCKER modules implemented in Discovery Studio 2017 R2 Client. We achieved 5 potential compounds according to the consensus analysis on seven different scoring functions and visual inspection (Figure S1). By the validation with the enzymatic assay, we found that MK inhibited the activity of FXIa.

MK's inhibitory potency and specificity

MK's inhibition on the proteolytic activities of FXIa and 9 homologous serine proteases were determined by chromogen-based enzymatic experiments (Figure 2A and 2B) [22]. These proteases include 5 coagulation proteases (FXIa, thrombin, FXa, FXIIa, and FVIIa) and 5 fibrinolytic proteases (plasmin, uPA, tPA, matriptase, and PK) (Table S2). MK inhibited FXIa with an IC_{50} value of 0.17±0.04 μM. In contrast, MK showed non-measurable inhibition against other serine proteases (IC_{50} > 100 μM), except PK (IC_{50}= 26.7±0.5 μM) and tPA (IC_{50}= 6.1±0.3 μM) (Figure 2B). Notably, the bleeding tendency of most clinical anticoagulants is because of the inhibition on the activity of thrombin or FXa. MK did not inhibit thrombin or FXa suggesting the low hemorrhagic risks.

Molecular mechanism of MK's inhibition and specificity

To reveal the molecular mechanisms of MK's inhibitory potency and selectivity, we performed molecular docking and atomistic MD simulations on the complexes of MK bound to FXIa, PK or FXa (Figure 3). The FXIa:MK complex was structurally stable and showed no large conformational changes over 500 ns, i.e. the root-mean-square deviation (RMSD) of MK was constantly below 1.5 Å, in contrast to the RMSDs of MK bound to PK or FXa fluctuating 1.5-3.0 Å (Figure S2A), suggesting the higher stability of MK:FXIa complex. Such distinctive dynamic features were also supported by the superimpositions of time course snapshots obtained from MD simulations (Figure 3A-C). Notably, MK stably persisted within the active site of FXIa with one dominant conformation, while the superimposed MK in PK and FXa showed varied conformational states, which aligned with the weak affinity determined by enzymatic experiments (Figure 2B). Thus, the virtual stability analysis was in agreement with our experimental determinations.

Figure 3D-F depicted the binding poses of MK to FXIa, FXa and PK, respectively. In both FXIa:MK and PK:MK complexes, MK's chloroquinoline P1 moiety deeply inserted into the S1 pocket, anchored by halogen bond and halogen-π interactions between the chloride atom and the phenolic group of Y228. In

contrast, MK failed to establish such interaction with FXa. Detailed structural comparisons suggested that the failure may be due to the occlusion by the indole ring of W215 which was engaged in stacking interactions with Y99, F174 and one phenyl ring of MK (Figure 3G and 3H). Compared to FXIa and PK, the W215 indole ring in FXa was flipped by ~120º (from -60º to 60º, Figure 3I), so that its sidechain directed toward the 2-phenylpropan-2-ol moiety of MK, making the chloroquinoline moiety stuck at the rim of S1 pocket. Intriguingly, bimodal distribution of the flipping dihedral angle (C-Cα-Cβ-Cγ of W215) was observed in the PK:MK complex. Such dihedral angle significantly increased from -60º to 60º at ~120 ns and then sharply decreased back to -60º at ~300 ns (Figure S3A). The distance between the phenyl ring of 2-phenylpropan-2-ol moiety of MK and the indole ring of W215 also exhibited large fluctuations at the same time periods (Figure S3B). Therefore, the formation of stacking interaction between W215 and MK is closely related to the flipping rotation of W215 sidechain. As a result, the co-existed flipped conformation of W215 in the PK:MK complex disrupted the stability of chloroquinoline moiety at the S1 pocket (Figure S3C). Consistently, the halogen-related interactions in FXIa:MK were stronger than those in PK:MK, as indicated by the plots of the centre-of-mass distance between the phenolic group of Y228 and the chloride atom (Figure 3J). Besides, the reduced stability of chloroquinoline moiety may also attribute to the loss of additional hydrogen bond formed with one of the catalytic triad residue S195. Furthermore, two additional hydrogen bonds were established with K192 and Y143 in FXIa, providing the desired boost in binding affinity.

MK inhibited the FXIa-induced clot formation *in vitro*

We next evaluated MK's effect on clot formation in human plasma with an addition of recombinant FXIa (Figure 2C). Citrate-stored plasma was pre-incubated with 5 nM recombinant FXIa and MK (0-25 μM) for 15 min. Clot formation was monitored by real-time determining the absorbance at 405 nm (A405) after the addition of 2 mM $CaCl_2$. The time to reach half of the plateau ($T_{1/2}$) was used to evaluate the anticoagulative effect of MK (Figure 2D). $T_{1/2}$ of normal plasma (the control group) was 9.5±1.3 min, which was significantly shortened till 4.6±0.1 min by the addition of FXIa. The presence of 1, 5, or 25 μM MK delayed clot formation, and $T_{1/2}$ was prolonged to 5.4±0.1, 7.5±0.6, or 8.3±0.8 min, respectively. This result demonstrates the inhibition of the FXIa-induced coagulation by MK.

MK suppressed the $FeCl_3$-stimulated carotid artery thrombosis *in vivo*

The *in vivo* antithrombotic properties of MK were evaluated in three thrombotic mouse models *in vivo*. For comparison, we parallelly studied the effects of two clinically prescribed oral anticoagulants, Warfarin and Apx (Figure 1B). First, we studied the antithrombotic effects of these anticoagulants in an $FeCl_3$-stimulated carotid artery thrombosis mouse model (Figure 4A-B). Saline, MK, warfarin, or Apx were administered (p.o.) 3-h before the aesthetic mice's carotid arteries were exposed and treated with a filter paper saturated with 6% $FeCl_3$ to trigger clot formation. Blood flow was real-time imaged and recorded by a laser speckle imaging instrument. The time-to-occlusion (TTO) was recorded to quantitatively compare the vascular occlusion among different groups. TTO in the untreated group was 287 s, which was prolonged to 363 s (P<0.05) or 678 s (P<0.01) by the administration with 2 mg/kg or 10 mg/kg MK,

respectively. Administration with 4 mg/kg warfarin or 10 mg/kg Apx increased TTO to 512 s (non-statistical significance) or 642 s (P<0.05), respectively. Warfarin was administered at a low dose (4 mg/kg) because of its high toxicity to mice [23].

MK suppressed electricity-stimulated carotid artery thrombosis *in vivo*

The antithrombotic properties of MK, Warfarin, and Apx were also evaluated in the electricity-stimulated carotid artery thrombosis mouse model (Figure 4C). Similarly, all anticoagulants were administered (p.o.) 3-h before the surgical exposure of the carotid artery and the stimulation with 0.1 mA electricity. The blood flow was real-time recorded by an infrared detector immediately after stimulation. TTO was recorded when the blood flow went below 5% and continuously kept for >5 s. The vessels of the untreated mice were occluded at 82 s after stimulation. With the administration of 4 mg/kg warfarin, 2 mg/kg, or 10 mg/kg Apx, the TTO was prolonged to 160 s (P<0.01), 145 s (non-statistical significance), or 210 s (P<0.05), respectively. Administration with 2 mg/kg or 10 mg/kg MK significantly delayed the vascular occlusion by increasing TTO until 135 s (P<0.05) or 202 s (P<0.01), respectively. Thus, in both carotid artery thrombotic models, MK performed antithrombotic effects comparable to those of the two mostly prescribed anticoagulants.

MK ameliorated the LPS-induced pulmonary micro-thrombus formation *in vivo*

We next evaluated the antithrombotic effects of MK, Warfarin, or Apx on inflammation-induced pulmonary micro-thrombus formation *in vivo*. The thrombosis in pulmonary vessels was stimulated by intraperitoneal injection with LPS in mice. Four hours before LPS-stimulation, mice were orally administrated with saline, MK (2 or 10 mg/kg), Warfarin (4 mg/kg), or Apx (10 mg/kg), respectively. One group without LPS-stimulation was set as the normal group for comparison. Four hours after stimulation, mice were sacrificed, and the lungs and blood were harvested for histopathological analysis and the determination of cytokine levels, respectively (Figure S4). Pulmonary histopathological analysis demonstrated that LPS-stimulation caused severe inflammation and thrombosis in lungs from the saline-treated group (Figure 5A). Treatments with MK, Warfarin, or Apx all ameliorated the micro-thrombi formation (Figure 5B-E). All the treated groups showed significantly reduced numbers and sizes of thrombi compared to the saline-treated group (Figure 5F). We also evaluated the effects of MK, Warfarin, or Apx on the inflammation levels by determining the plasma levels of IL-1β or TNF-α (Figure 5G-H). Consistent with the known anti-inflammatory effects of MK [24, 25, 26], administration with 10 mg/kg MK reduced the levels of both IL-1β and TNF-α to the normal levels. However, despite Warfarin and Apx ameliorated pulmonary thrombosis, they did not show anti-inflammatory effects. The decreased TNF-α level by Warfarin was by impairing the transcription of TNF-α rather than by anti-inflammatory property [27, 28]. Thus, based on its anti-inflammatory and antithrombotic properties, MK might exhibit a dual therapeutic effects on pathologies combining inflammation and thrombosis, e.g. sepsis-induced disseminated intravascular coagulation (DIC).

MK caused mild hemorrhage *in vivo*

Next, we evaluated the potential hemorrhage caused by MK, Warfarin, and Apx using a tail-truncation mouse model (Figure 6). Both bleeding time and hemoglobin loss were recorded. Compared to the saline-treated mice, Mice treated with 4 mg/kg warfarin showed a doubled bleeding time and a 3.7-fold enhanced hemoglobin. In contrast, neither MK nor Apx increased the bleeding time at the dose of 10 mg/kg. At the concentration of 50 mg/kg, MK and Apx prolonged the bleeding time for 1.46-fold and 1.35-fold, respectively. However, although Apx- and MK-treated mice showed similar bleeding time (Figure 6A), MK caused much lower hemoglobin loss than Apx did (Figure 6B): At the concentrations of 10 and 50 mg/kg, MK only caused around 1.3-fold enhanced hemoglobin loss compared to the saline-treated group. In contrast, at the same concentrations, Apx caused 2.9- and 3.5-fold enhanced hemoglobin loss, respectively. This result indicates that, compared to VAKs or DOACs, MK, as a FXIa inhibitor, does not impair the hemostatic function and causes much milder hemorrhage, which is also consistent with the fact that mild bleeding is a rare side-effect of MK.

MK did not affect the global coagulation

The influences of MK on global coagulation were evaluated by determining prothrombin time (PT), activated partial thromboplastin time (APTT), and thromboelastographic parameters in plasma from heathy individuals (Table 1). MK showed non-measurable effect on all of the tested parameters even at a high concentration up to 1000 μM (>5000-fold IC_{50}), indicating that MK did not compromise the normal hemostatic function. Theoretically, the intervention with the intrinsic coagulation pathway was considered to prolong or shorten APTT [29]. Many FXI(a) inhibitors have been reported to prolong APTT [30]. However, increasing evidence has demonstrated the poor correlation of APTT with plasma FXI(a) activities/levels [31]. A high portion of patients with FXI-deficiency, especially the ones with moderate deficiency (>20% of normal level), showed normal APTT [32, 33]. Besides, the influences of FXIa inhibitors on APTT also vary significantly. For instance, MAA868, a monoclonal antibody developed by Novartis, showed an $APTT_{EC2\times}$ concentration >3000-fold higher than its K_i value [34]. Similarly, a pyrimidine-based FXIa inhibitor showed an $APTT_{EC1.5\times}$ concentration ~5000-fold higher than its IC_{50} value [35]. Sullenger et al. identified two RNA aptamers with identical K_i values of inhibiting FXIa (60 and 63 nM). However, at the same concentration, one aptamer doubled the APTT in human plasma, but the other one showed non-obvious influence [36]. Thus, APTT might not be a good indicator for the evaluation of the efficacies of FXIa inhibitors.

MK suppressed coagulations in clinical plasma samples

Thrombophilia is dangerous because blood has a high tendency to coagulate in vessels. We evaluated the effects of MK on the coagulation of 20 clinical hypercoagulable plasma samples which showed shortened APTT and enhanced D-dimer levels (Table S3). These plasma samples were collected from individuals in different situations, e.g. late pregnancy, hypotension, acute myocardial infarction (AMI), etc. $CaCl_2$ was used to trigger the coagulation in the samples with or without 25 μM MK. Coagulation was monitored by real-time recording A405 (Figure 7A-B). The amount of fibrin generation was quantitatively

represented by the plateaued A405 subtracting the starting A405 (A_{405}(+MK) or A_{405}(-MK)) (Figure 7A). The time when clot formation reached half of the plateau was recorded as $T_{1/2}$(+MK) or $T_{1/2}$(-MK). The value of A_{405}(-MK)-A_{405}(+MK) represented the influence of 25 μM MK on fibrin generation: positive and negative values indicate the reduced and increased fibrin generation, respectively (Figure 7C). Similarly, the value of $T_{1/2}$(+MK)-$T_{1/2}$(-MK) indicates the influence of MK on the clotting time: positive and negative values indicate the prolonged and reduced clotting time, respectively (Figure 7D).

The effects of MK on the clotting time in different hypercoagulable samples varied significantly (Figure 7D). MK prolonged the clotting times in 12 samples while shortened those in the other 8 samples. In contrast, MK inhibited the amount of fibrin generation in all 20 samples (Figure 7C), although the reduced ranges varied. These results are consistent with the complex roles of FXI(a) in coagulation. The clinical phenotypes in FXI-deficient patients are variable, and have poor correlation with the baseline FXI(a) activity [37]. Apx completely inhibited the clot formation in all samples (Figure S5), because the inhibition of FXa directly inhibited the generation of thrombin (Figure S4). In contrast, MK, a selective FXIa inhibitor, only reduced the amount of fibrin generation, which is consistent with the less important role of FXI(a) in normal coagulation (hemostasis). In such *in vitro* setup, the inhibition of FXIa only reduced the amplification of thrombin generation while had no effect on existing thrombin. Besides, the inhibition of TFPI by FXIa does not affect the already generated thrombin either. Thus, FXIa is not essential in the *in vitro* coagulation, while can be critical for thrombosis, because thrombosis needs resistance against anticoagulation and fibrinolysis *in vivo*[38]. Thus, although MK did not completely suppress clot formation like Apx did *in vitro*, our animal models demonstrated the close antithrombotic efficacies of MK and Apx.

Discussion

In this study, we employed an *in silico* structure-based approach to screen a drug repurposing library and successfully identified MK as a potent and selective inhibitor of FXIa. MK was originally developed for treating asthma, a paroxysmal airflow obstruction caused by chronic airway inflammation. Historically, asthma was considered irrelevant to thrombosis, which normally occurs within blood vessels. As the cross-talk between coagulation and inflammation is now being revealed, increasing evidence has demonstrated that fibrin formation in pulmonary compartments and the upper airway can be important in asthmatic development [39]. First, fibrin assembles with mucus forming plugs obstructing the airway. In addition, fibrinogen cleavage products (FCPs), generated from the cleavage by either fungal proteases or thrombin, can trigger the toll-like receptor 4 signaling pathway in epithelial cells leading to inflammation and thus boosting the generation of eosinophilia and mucus in the airway [40]. Besides, patients with asthma showed 2-5-fold higher risk of pulmonary embolism compared to the general population [41]. FXI(a) is responsible for the generation of thrombin and thus may also associate with the aggravation of asthmatic symptoms. The marketed antiasthmatic drug, MK, was originally developed to block leukotriene receptors and inhibit smooth muscle contraction. Thus, MK's antiasthmatic function might also be relevant to its anticoagulative effect revealed in this study.

Because of the interactions with foods and drugs, VKAs have caused the highest incidence of drug-related life-threatening events [5, 42]. In contrast, no drug interactions have been reported for MK suggesting a more versatile drug/food combination. After its approval in 1998, MK show generally mild adverse effects according to the post-marketing surveillance [43]. However, leukotriene modulators are associated with increased incidences of agitation, aggression, anxiousness, irritability, or even suicidal behaviors [44]. Accordingly, US-FDA required a boxed warning for MK to strengthen an existing warning about the risk of neuropsychiatric events [45]. Thus, although MK overcomes the main problems of typical anticoagulants, hemorrhage and interactions with drugs/foods, the neuropsychiatric risk might hinder the long-term administration of MK. However, its well-studied pharmacology and toxicology may be beneficial to exploratory researches on the off-label antithrombotic use of MK.

It seems to be a coincidence that MK can simultaneously inhibit FXIa and cys-LTRs. The crystal structures of cys-LTR-1 in complexes with two leukotriene antagonists were recently reported [46]. Based on the large difference in the structures of cys-LTR-1 and FXIa, MK can be engineered to enhance its inhibitory potency against FXIa promoting antithrombotic efficacy, and to reduce its affinity to cys-LTRs ameliorating neuropsychiatric risk. Thus, MK can be a promising lead compound for generating more potent oral anticoagulants with low hemorrhagic and neuropsychiatric risks.

Our *in silico* models suggested that the neutral chlorinated aromatic ring at the P1 moiety is pivotal for MK's inhibitory activity. Similar moieties have been also successfully applied in the structures of oral inhibitors of FXIa [47], FXa [48, 49], and thrombin [50]. Based on structural comparisons, we found that the sidechain orientation of W215 may be a major determinant for the selectivity of MK. The flexibility of W215 segment is an intrinsic nature of trypsin-like protease and the conformational state of W215 determines the accessibility of substrates or ligands to the S1 pocket [51, 52]. Previous crystallographic analysis and biochemical assays indicated that W215 may exist in two conformational states (open and closed), which can be allosterically regulated by distal residues [53]. Consistent with this scenario, we observed that the binding of specific compounds, like MK investigated here, may selectively turn on the switch of W215 conformation, which then inversely controls the stability of compound binding. It seems that the extent of conformational change is dependent on particular amino acids around W215 as well as the tendency for interaction between the compound and W215. Therefore, it provides a novel strategy for the design of FXIa-targeted anticoagulants by selectively regulating the conformation of key active site residues.

In this study, by a high-throughput virtual screening, we identified MK as a potent and selective inhibitor of FXIa, a safer antithrombotic target compared to (pro)thrombin and FX(a). MD simulations elucidated its mechanisms of the inhibition and specificity. The subsequent *in vitro* and *in vivo* evaluations demonstrated that the antithrombotic effects of MK were comparable to those of clinical anticoagulants, Warfarin and Apxaban. More importantly, MK caused obviously milder hemorrhage than Warfarin or Apxaban did, indicating its higher safety. In addition, MK did not affect APTT in plasma from healthy individuals but suppressed clot formation in plasma from clinical hypercoagulable patients. This study

demonstrates the potent and safe antithrombotic effect of MK and reports a new scaffold for developing anticoagulants targeting FXIa.

Methods

General. Animal experiments were approved by the Animal Ethics Committee of the College of Biological Science and Engineering, Fuzhou University (2019-SG-006) and carried out in accordance with the guidelines. Male institute of cancer research (ICR) Mice (6-8 weeks) were purchased from SLAC Laboratory Animal Co., Ltd (Shanghai, China). The use of clinical samples was approved by the Ethics Committees of Sanming First Hospital Affiliated to Fujian Medical University. The detailed sources of compounds, chemicals, recombinant protein, and manufacturers were listed in the Supplementary Methods (Table S1).

***In silico* screening and MD simulation.** Structural preparation, molecular docking, and consensus scoring were all carried out with Discovery Studio (DS 2017R2) package (BIOVIA, San Diego, USA). All-atom MD simulations were carried out on MK bound to FXIa, PK, and FXa using Amber 16 package[54]. The details of MD simulations are fully outlined in the Supplementary Methods.

Arterial thrombosis mouse model stimulated by $FeCl_3$ or electricity. ICR Mice (male, 6-8 weeks) were administered (p.o.) with saline, MK, Warfarin or Apx (N=6) 3-h before the left carotid arteries of the anesthetized mice were exposed and treated with a piece of filter paper saturated with 6% $FeCl_3$ or 0.1 mA current to induce thrombosis. Once thrombosis was stimulated, the bloodstream of $FeCl_3$-stimulated and electricity-stimulated mice was monitored by Laser Speckle Contrast Imaging System and an YLS-14B animal thrombus formation instrument, respectively. The occlusive rate (%) of carotid blood was recorded every 4 seconds. The times to occlusion (vascular occlusive rate reached 95%) were recorded.

LPS-induced pulmonary microvascular thrombotic mouse model. Lipopolysaccharides (LPS)-induced pulmonary microvascular thrombotic mouse model was established by intraperitoneal (i.p.) injections with 250 μg/kg LPS and 500 mg/kg D-(+)-Galactosamine in ICR mice (male, 6-8 weeks) [55]. Mice were randomly divided into 6 groups (6 mice per group). One group without stimulation was set as the normal group. The rest 5 groups were administered (p.o.) with saline, 2, 10 mg/kg MK, 4 mg/kg Warfarin or 10 mg/kg Apx 3-h before LPS-stimulation. 4-h after stimulation, mice were anesthetized and sacrificed. The blood and lungs were harvested. Blood concentrations of IL-1β and TNF-α, were determined by enzyme-linked immunosorbent assay (ELISA) kits. Histopathological sections of lungs were stained with hematoxylin and eosin (H&E) and photographed at a magnification of 200× imaged by a Leica DMi8 inverted microscope. The numbers of microthrombi were counted in 6 histopathological sections from 3 mice in each group, and the areas of the microthrombi were determined by the software of Image J.

Tail transection mouse model. Tail bleeding time was determined as described previously with slight modifications [56]. Mice were p.o. administered with saline, 10, 50 mg/kg MK, 4 mg/kg Warfarin, 10 and 50 mg/kg Apx (6 mice per group), 3 h before the tails were transected 10 mm from the tip. The transected

tails were immediately immersed in 10 ml isotonic saline at 37 °C. The bleeding time was recorded once the bleeding stopped. The blood loss was quantified by measuring the haemoglobin content collected in the 10 ml isotonic saline. After centrifugation, erythrocytes were collected and lysed with 2 mL lysis buffer (8.3 g/L NH_4Cl, 1 g/L $KHCO_3$, and 0.037 g/L EDTA). The A575 of each sample was determined.

Statistical analysis. The statistical significance was analyzed by using 1-way ANOVA followed by Bartlett test. A *P* value of less than 0.05 was considered statistically significant.

Declarations

Acknowledgements

This work was financially supported by grants from the Natural Science Foundation of Fujian Province (2019J06007, 2018J05031 and 2018J01729); the National Key R&D Program of China (2017YFE0103200); the National Natural Science Foundation of China (21708043). The authors gratefully acknowledge the computing time granted by the Fujian Supercomputing Center.

Author contributions

D.W., Y.Z., M.S., H.L., and D.Z. carried out experiments; Y.Q., H.Y., and J.L. carried out virtual screening and MD simulations; C.L., M.H.(Meijuan Huang), L.J., C.Y., Y.C., and M.H. (Mingdong Huang) provided technical supports; J.L. and P.X. designed the project and wrote the manuscript; C.L. and M.H. edited manuscript.

Competing interests

The authors declare no competing financial interests.

References

1. Mackman N. Triggers, targets and treatments for thrombosis. *Nature* **451**, 914–918 (2008).
2. Ferland G. The discovery of vitamin K and its clinical applications. *Ann Nutr Metab* **61**, 213–218 (2012).
3. Koscielny J, Rosenthal C, von Heymann C. Update on Direct Oral AntiCoagulants (DOACs). *Hamostaseologie* **37**, 267–275 (2017).
4. Chan NC, Weitz JI. Antithrombotic Agents. *Circ Res* **124**, 426–436 (2019).
5. Di Minno A, *et al.* Old and new oral anticoagulants: Food, herbal medicines and drug interactions. *Blood Rev* **31**, 193–203 (2017).
6. Puy C, Rigg RA, McCarty OJ. The hemostatic role of factor XI. *Thromb Res* **141 Suppl 2**, S8-S11 (2016).

7. Gailani D, Bane CE, Gruber A. Factor XI and contact activation as targets for antithrombotic therapy. *J Thromb Haemost* **13**, 1383–1395 (2015).
8. Woodruff RS, Sullenger B, Becker RC. The many faces of the contact pathway and their role in thrombosis. *J Thromb Thrombolysis* **32**, 9–20 (2011).
9. Meijers JC, Tekelenburg WL, Bouma BN, Bertina RM, Rosendaal FR. High levels of coagulation factor XI as a risk factor for venous thrombosis. *N Engl J Med* **342**, 696–701 (2000).
10. Siegerink B, Govers-Riemslag JW, Rosendaal FR, Ten Cate H, Algra A. Intrinsic coagulation activation and the risk of arterial thrombosis in young women: results from the Risk of Arterial Thrombosis in relation to Oral contraceptives (RATIO) case-control study. *Circulation* **122**, 1854–1861 (2010).
11. Doggen CJ, Rosendaal FR, Meijers JC. Levels of intrinsic coagulation factors and the risk of myocardial infarction among men: Opposite and synergistic effects of factors XI and XII. *Blood* **108**, 4045–4051 (2006).
12. Mohammed BM, *et al.* An update on factor XI structure and function. *Thromb Res* **161**, 94–105 (2018).
13. Mackman N, Bergmeier W, Stouffer GA, Weitz JI. Therapeutic strategies for thrombosis: new targets and approaches. *Nat Rev Drug Discov* **19**, 333–352 (2020).
14. Puy C, *et al.* Activated factor XI increases the procoagulant activity of the extrinsic pathway by inactivating tissue factor pathway inhibitor. *Blood* **125**, 1488–1496 (2015).
15. Flaumenhaft R. Making (anti)sense of factor XI in thrombosis. *N Engl J Med* **372**, 277–278 (2015).
16. DeLoughery EP, Olson SR, Puy C, McCarty OJT, Shatzel JJ. The Safety and Efficacy of Novel Agents Targeting Factors XI and XII in Early Phase Human Trials. *Semin Thromb Hemost* **45**, 502–508 (2019).
17. Thomas D, *et al.* BAY 1213790, a fully human IgG1 antibody targeting coagulation factor XIa: First evaluation of safety, pharmacodynamics, and pharmacokinetics. *Res Pract Thromb Haemost* **3**, 242–253 (2019).
18. Wermuth HR, Badri T, Takov V. Montelukast. In: *StatPearls*) (2020).
19. Sun W, Liu HY. Montelukast and Budesonide for Childhood Cough Variant Asthma. *J Coll Physicians Surg Pak* **29**, 345–348 (2019).
20. Sanchez G, Buitrago D. Effect of Montelukast 10 mg in Elderly Patients with Mild and Moderate Asthma Compared with Young Adults. Results of a Cohort Study. *Open Respir Med J* **12**, 67–74 (2018).
21. Peng WS, Chen X, Yang XY, Liu EM. Systematic review of montelukast's efficacy for preventing post-bronchiolitis wheezing. *Pediatr Allergy Immunol* **25**, 143–150 (2014).
22. Wang D, *et al.* Suppression of Tumor Growth and Metastases by Targeted Intervention in Urokinase Activity with Cyclic Peptides. *J Med Chem* **62**, 2172–2183 (2019).
23. Zhang H, *et al.* Inhibition of the intrinsic coagulation pathway factor XI by antisense oligonucleotides: a novel antithrombotic strategy with lowered bleeding risk. *Blood* **116**, 4684–4692

(2010).

24. Hamamoto Y, Ano S, Allard B, O'Sullivan M, McGovern TK, Martin JG. Montelukast reduces inhaled chlorine triggered airway hyperresponsiveness and airway inflammation in the mouse. *Br J Pharmacol* **174**, 3346–3358 (2017).
25. Dong H, *et al.* Montelukast inhibits inflammatory response in rheumatoid arthritis fibroblast-like synoviocytes. *Int Immunopharmacol* **61**, 215–221 (2018).
26. Davino-Chiovatto JE, *et al.* Montelukast, Leukotriene Inhibitor, Reduces LPS-Induced Acute Lung Inflammation and Human Neutrophil Activation. *Arch Bronconeumol* **55**, 573–580 (2019).
27. Belij S, *et al.* Effects of subacute oral warfarin administration on peripheral blood granulocytes in rats. *Food Chem Toxicol* **50**, 1499–1507 (2012).
28. Kater AP, Peppelenbosch MP, Brandjes DP, Lumbantobing M. Dichotomal effect of the coumadin derivative warfarin on inflammatory signal transduction. *Clin Diagn Lab Immunol* **9**, 1396–1397 (2002).
29. Winter WE, Flax SD, Harris NS. Coagulation Testing in the Core Laboratory. *Lab Med* **48**, 295–313 (2017).
30. Al-Horani RA. Factor XI(a) inhibitors for thrombosis: an updated patent review (2016-present). *Expert Opin Ther Pat* **30**, 39–55 (2020).
31. Wheeler AP, Gailani D. Why factor XI deficiency is a clinical concern. *Expert Rev Hematol* **9**, 629–637 (2016).
32. Salloum-Asfar S, *et al.* Assessment of two contact activation reagents for the diagnosis of congenital factor XI deficiency. *Thromb Res* **163**, 64–70 (2018).
33. Puetz J, Hugge C, Moser K. Normal aPTT in children with mild factor XI deficiency. *Pediatr Blood Cancer* **65**, (2018).
34. Koch AW, *et al.* MAA868, a novel FXI antibody with a unique binding mode, shows durable effects on markers of anticoagulation in humans. *Blood* **133**, 1507–1516 (2019).
35. Corte JRL, NJ, US), De Lucca, Indawati (Pennington, NJ, US), Fang, Tianan (Levittown, PA, US), Yang, Wu (Princeton Junction, NJ, US), Wang, Yufeng (North Brunswick, NJ, US), Dilger, Andrew K. (Ewing, NJ, US), Pabbisetty, Kumar Balashanmuga (Piscataway, NJ, US), Ewing, William R. (Yardley, PA, US), Zhu, Yeheng (Stockton, NJ, US), Wexler, Ruth R. (Belle Mead, NJ, US), Pinto, Donald J. P. (Churchville, PA, US), Orwat, Michael J. (New Hope, PA, US), Smith II, Leon M. (Somerset, NJ, US). MACROCYCLES WITH AROMATIC P2' GROUPS AS FACTOR XIA INHIBITORS. United States (2017).
36. Woodruff RS, Ivanov I, Verhamme IM, Sun MF, Gailani D, Sullenger BA. Generation and characterization of aptamers targeting factor XIa. *Thromb Res* **156**, 134–141 (2017).
37. Santoro C, *et al.* Bleeding phenotype and correlation with factor XI (FXI) activity in congenital FXI deficiency: results of a retrospective study from a single centre. *Haemophilia* **21**, 496–501 (2015).
38. Kazmi RS, Boyce S, Lwaleed BA. Homeostasis of Hemostasis: The Role of Endothelium. *Semin Thromb Hemost* **41**, 549–555 (2015).

39. Perrio MJ, Ewen D, Trevethick MA, Salmon GP, Shute JK. Fibrin formation by wounded bronchial epithelial cell layers in vitro is essential for normal epithelial repair and independent of plasma proteins. *Clin Exp Allergy* **37**, 1688–1700 (2007).
40. Lambrecht BN, Hammad H. Asthma and coagulation. *N Engl J Med* **369**, 1964–1966 (2013).
41. Majoor CJ, *et al.* Risk of deep vein thrombosis and pulmonary embolism in asthma. *Eur Respir J* **42**, 655–661 (2013).
42. Ageno W, Gallus AS, Wittkowsky A, Crowther M, Hylek EM, Palareti G. Oral anticoagulant therapy: Antithrombotic Therapy and Prevention of Thrombosis, 9th ed: American College of Chest Physicians Evidence-Based Clinical Practice Guidelines. *Chest* **141**, e44S-e88S (2012).
43. Calapai G, Casciaro M, Miroddi M, Calapai F, Navarra M, Gangemi S. Montelukast-induced adverse drug reactions: a review of case reports in the literature. *Pharmacology* **94**, 60–70 (2014).
44. Kovesi T. Neuropsychiatric side effects of montelukast. *J Pediatr* **212**, 248 (2019).
45. In brief: Neuropsychiatric events with montelukast. *Med Lett Drugs Ther* **62**, 65 (2020).
46. Luginina A, *et al.* Structure-based mechanism of cysteinyl leukotriene receptor inhibition by antiasthmatic drugs. *Sci Adv* **5**, eaax2518 (2019).
47. Pinto DJ, *et al.* Structure-based design of inhibitors of coagulation factor XIa with novel P1 moieties. *Bioorg Med Chem Lett* **25**, 1635–1642 (2015).
48. Perzborn E, Roehrig S, Straub A, Kubitza D, Misselwitz F. The discovery and development of rivaroxaban, an oral, direct factor Xa inhibitor. *Nat Rev Drug Discov* **10**, 61–75 (2011).
49. Kohrt JT, *et al.* The discovery of (2R,4R)-N-(4-chlorophenyl)-N- (2-fluoro-4-(2-oxopyridin-1(2H)-yl)phenyl)-4-methoxypyrrolidine-1,2-dicarboxamide (PD 0348292), an orally efficacious factor Xa inhibitor. *Chem Biol Drug Des* **70**, 100–112 (2007).
50. Young MB, *et al.* Discovery and evaluation of potent P1 aryl heterocycle-based thrombin inhibitors. *J Med Chem* **47**, 2995–3008 (2004).
51. Pelc LA, Koester SK, Chen Z, Gistover NE, Di Cera E. Residues W215, E217 and E192 control the allosteric E*-E equilibrium of thrombin. *Sci Rep* **9**, 12304 (2019).
52. Chakraborty P, Di Cera E. Induced Fit Is a Special Case of Conformational Selection. *Biochemistry* **56**, 2853–2859 (2017).
53. Niu W, *et al.* Crystallographic and kinetic evidence of allostery in a trypsin-like protease. *Biochemistry* **50**, 6301–6307 (2011).
54. Casw DAB, R.M.; Botello-Smith, W.; Cerutti, D.S.; Cheatham, III, T.E.; Darden, T.A.; Duke, R.E.; Giese, T.J.; Gohlke, H.; Goetz, A.W.; et al. AMBER 2016.). University of California: San Francisco, CA, USA (2016).
55. Gao HF, Xiao GX, Ren JD, Xia PY. [Reproduction of the murine endotoxin shock model in D-galactosamine-sensitized KunMing mice]. *Zhonghua Shao Shang Za Zhi* **23**, 424–427 (2007).
56. Gong L, *et al.* A specific plasminogen activator inhibitor-1 antagonist derived from inactivated urokinase. *J Cell Mol Med* **20**, 1851–1860 (2016).

Table

Table 1: Conventional and viscoelastic coagulation tests in plasma from healthy individuals in the presence of different concentrations of MK. PT: prothrombin time, APTT: activated partial thromboplastin time, TEG parameters: R time: reaction time, K time: Kinetic time, Angle: slope of tracing that represents clot formation, MA: maximum amplitude of tracing, CI: coagulation index, LY30: clot lysis at 30 min following MA. All values are represented as mean ± SD (N = 3).

MK	0 µM	40 µM	200 µM	1000 µM	Reference
PT / s	14 ± 0.3	14 ± 0.5	12 ± 0.3	15 ± 0.2	11-14.3
APTT / s	34 ± 3.4	35 ± 2	32 ± 2	31 ± 0.5	33.7-40.3
R time / min	3.9 ± 0.29	4.2 ± 0.67	4.4 ± 0.69	4.2 ± 0.31	4-8
K time / min	1.7 ± 0.07	1.77 ± 0.18	2.1 ± 0.11	2.3 ± 0.16	1-3
Angle / degree	68 ± 0.4	66 ± 3	63 ± 1.5	59 ± 7.5	53-72
MA / mm	55 ± 2.1	55 ± 3.8	51 ± 4	51 ± 0.6	50-70
CI	0.87 ± 0.49	0.53 ± 1.0	-0.37 ± 0.96	-0.6 ± 0.53	-3-3
LY30	0.13 ± 0.04	0.1 ± 0	0.1 ± 0	0.33 ± 0.31	0-0.8

Figures

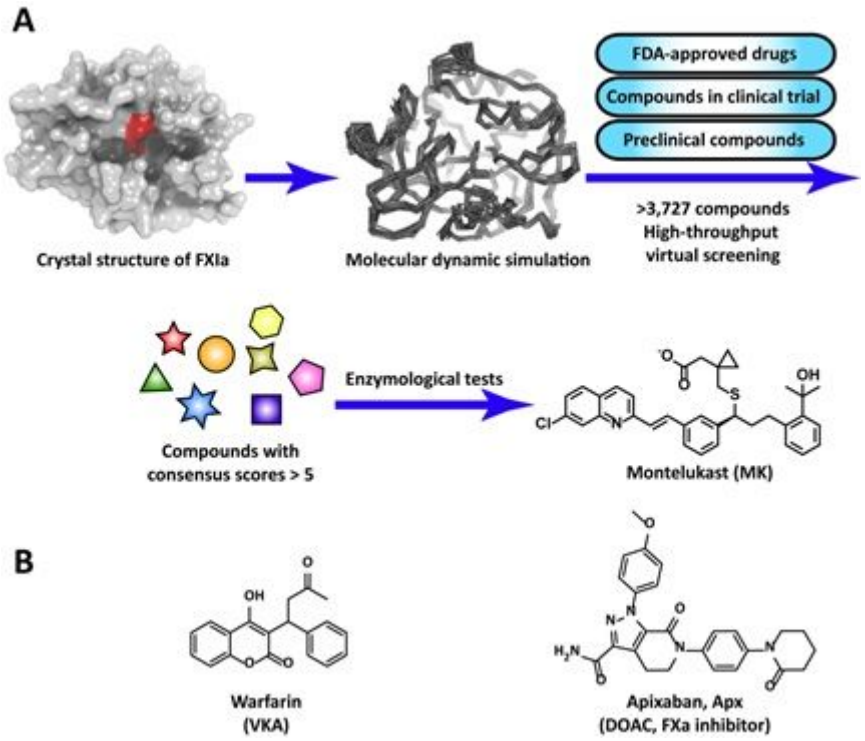

Figure 1

Structure-based discovery of MK as a potent FXIa inhibitor. (A) Scheme of the high-throughput virtual screening of FXIa inhibitor from a drug repurposing library including FDA-approved drugs, and compounds in clinical trials or preclinical studies. The chemical structure of MK was demonstrated. (B) Chemical structures of the two clinical anticoagulants used as the positive controls in this study: warfarin and Apx.

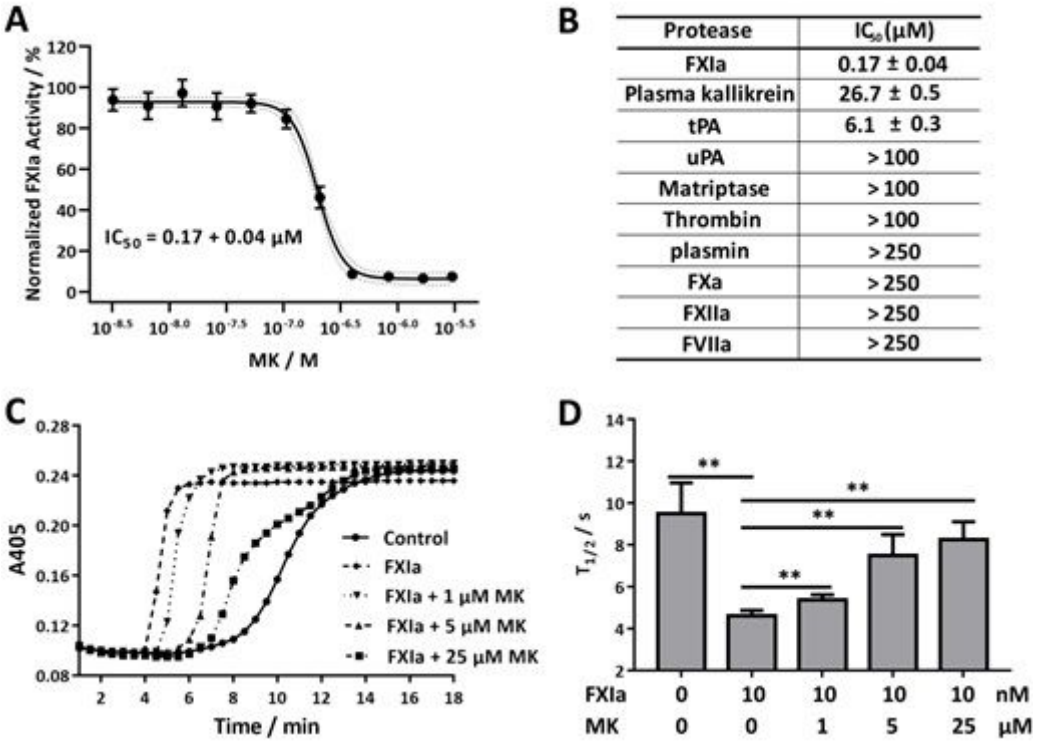

Protease	IC_{50} (μM)
FXIa	0.17 ± 0.04
Plasma kallikrein	26.7 ± 0.5
tPA	6.1 ± 0.3
uPA	> 100
Matriptase	> 100
Thrombin	> 100
plasmin	> 250
FXa	> 250
FXIIa	> 250
FVIIa	> 250

Figure 2

MK inhibited the proteolytic activity of FXIa and FXIa-induced clot formation in human plasma. (A) Regression curve of MK's inhibition against FXIa's proteolytic activity determined by chromogenic substrate S-2288. (B) IC50 values of MK's inhibition against FXIa and homologous proteases. PK: plasma kallikrein, tPA/uPA: tissue/urokinase-type plasminogen activator. (C) MK inhibited FXIa-induced clot formation in human plasma. Clot formation was monitored in real-time by determining A405. (D) The time to reach the half of the plateau (T1/2) in each curve in panel C. The values are represented as mean ± standard deviation (SD). **P < 0.01.

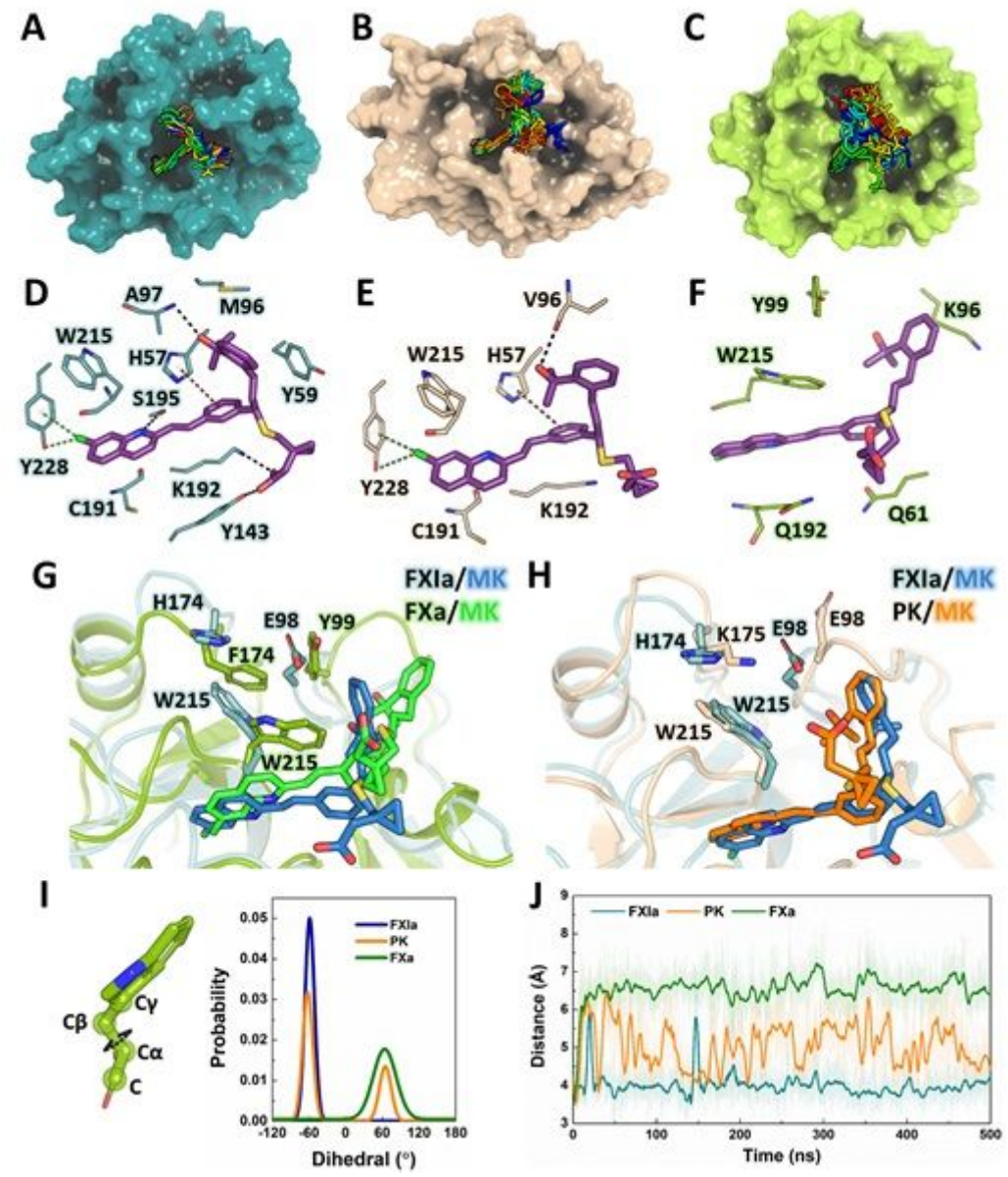

Figure 3

The inhibitory and selective mechanisms of MK revealed by MD simulations. A-C: The superimpositions of 20 snapshots of the MD simulations of MK bound to FXIa (A), PK (B), or FXa (C) collected every 25 ns. D-F: The binding modes of MK to FXIa (D), PK (E), or FXa (F) in the most representative structures of

corresponding MD simulations. Hydrogen bond and π-π stacking interactions were shown by black and red dashed lines, respectively. Halogen bond and halogen-π interactions were shown by green dashed lines. G, H: Superimpositions of the binding sites of MK in FXIa with the ones in FXa (G) and PK (H). I: The probability distributions of the dihedral angle among C-Cα-Cβ-Cγ of W215. J: The centre-of-mass distances between the chloride atom of MK and the phenolic group of Y228.

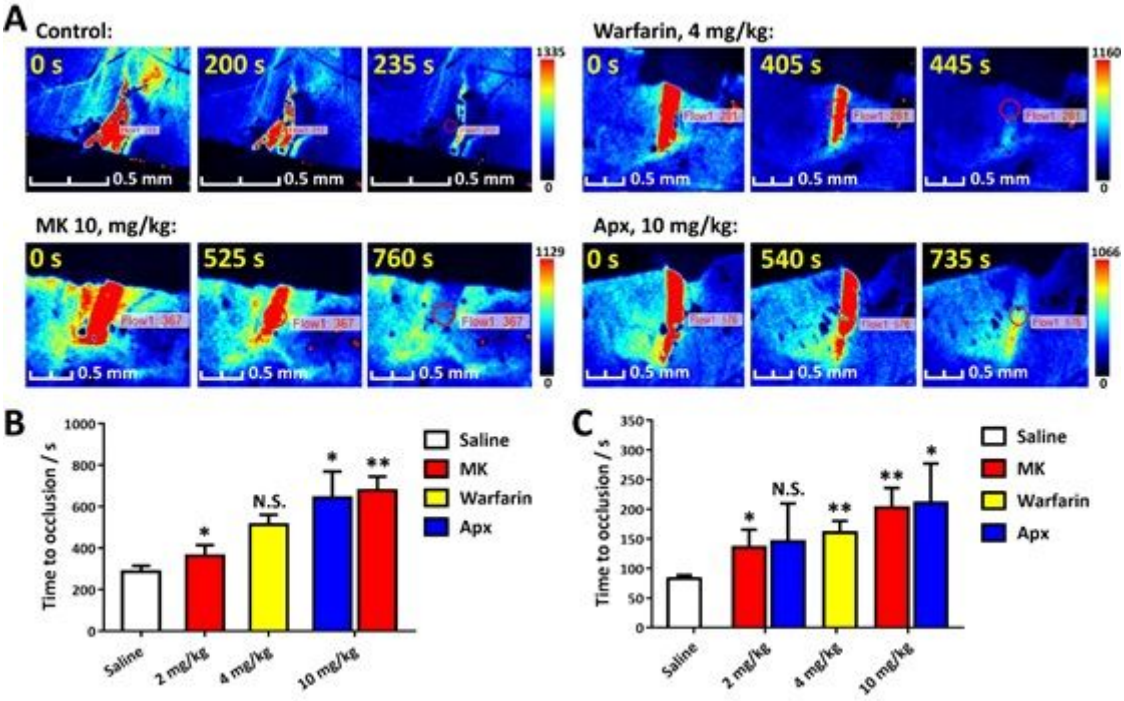

Figure 4

MK inhibited the carotid arterial thrombosis stimulated by FeCl3 (A-B) or electricity (C) in vivo. (A) Representative graphics of speckle-imaged blood flow in the carotid artery at various time points after FeCl3 stimulation. The mice were administered with saline, 10 mg/kg MK, 4mg/kg warfarin, or 10 mg/kg Apx, respectively. (B) The time to occlusion (TTO) in the carotid arteries of mice stimulated by FeCl3 in panel A. (C) The time to occlusion (TTO) in the carotid artery of mice stimulated by electricity administered by saline, 2 mg/kg, 10 mg/kg MK, 4 mg/kg warfarin, 2 mg/kg, or 10 mg/kg Apx. The values are represented as mean ± standard error of the mean (SEM). *P < 0.05, **P < 0.01, N.S.: no significance versus the saline-treated group (N=6).

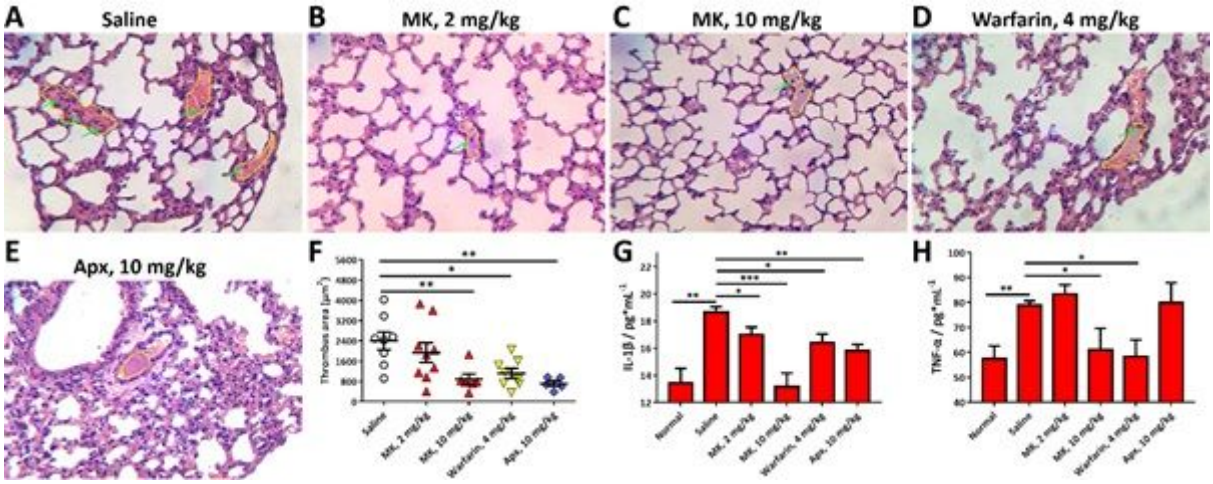

Figure 5

MK ameliorated inflammation and thrombosis in an LPS-induced septic model. A-E: Representative images of the H&E-stained histopathological sections of lungs from mice administrated (p.o.) with saline, MK (2 or 10 mg/kg), Warfarin (4 mg/kg), or Apx (10 mg/kg) 4-hour before LPS-stimulation, respectively. F: Quantification of the numbers and sizes of thrombi in lungs from the histopathological sections from LPS-stimulated mice in above groups. The quantification was based on one histopathological section from each mouse (3 mice per group). The yellow-highlight regions indicate pulmonary thrombi. The green arrows indicate leukocytes. G-H: Plasma concentrations of IL-1β (G) and TNF-α (H) in LPS-stimulated mice with the above administrations (N=6). The normal group indicates the mice in such group received neither anticoagulants nor LPS administration. The values are represented as mean ± SEM. *P < 0.05, **P < 0.01, ***P<0.001 versus the saline-treated group.

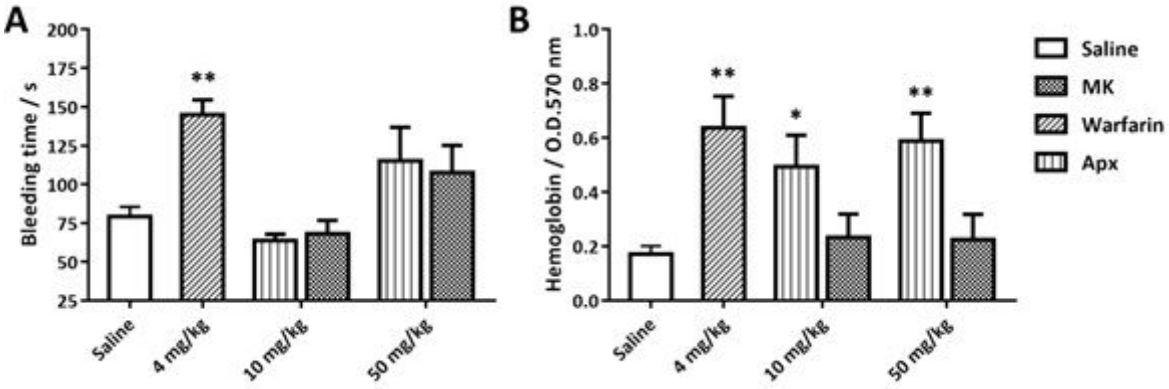

Figure 6

The hemorrhagic risks of MK, Warfarin, and Apx evaluated in a tail-truncation model. Mice were administered with saline, warfarin (4 mg/kg), MK (10 or 50 mg/kg), or Apx (10 or 50 mg/kg) 3 h before the tail-truncation. The bleeding time (A) and the hemoglobin loss (B) were recorded. The values are represented as mean ± SEM. *P < 0.05, **P < 0.01, versus the saline-treated group (N=6).

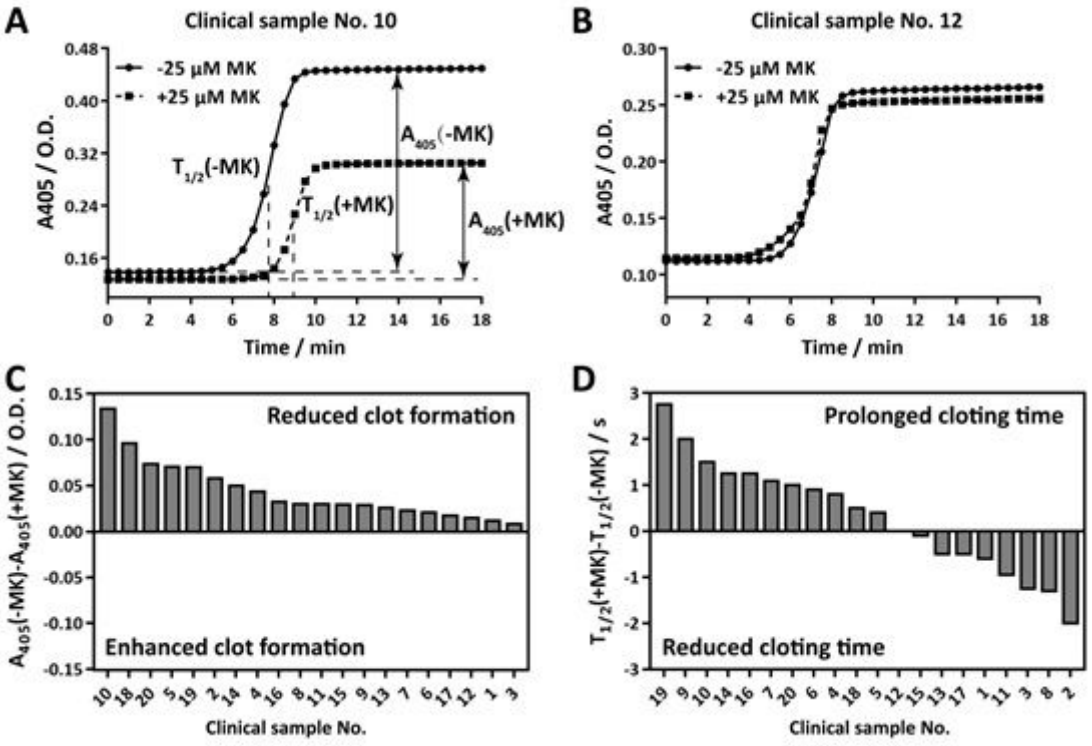

Figure 7

MK inhibited the clot formation in clinical hypercoagulable plasma samples. A-B: The curves of clot formation in clinical plasma sample No.10 and 12 in the presence or absence of 25 μM MK. 25 μM MK remarkably prolonged the clotting time and suppressed the fibrin deposition in sample No.10 (A), while had non-obvious effect on that in sample No.12 (B). The amount of fibrin deposition was indirectly represented by A405(-MK) or A405(+MK). The clotting time was represented by T1/2(-MK) or T1/2(+MK). C: The reduced or increased clot formation in 20 clinical plasma samples (A405(-MK)-A405(+MK)): The positive or negative values indicate the reduced or increased clot formation, respectively. D: The prolonged or shortened T1/2 of 20 clinical plasma samples by MK (T1/2(+MK)-T1/2(+MK)). The positive or negative values indicate the prolonged or shortened T1/2, respectively. The samples were arranged in the descending order. The detailed information of the sources of the 20 samples were listed in Table S2. The curves of other 18 patients were presented in Figure S6-8.

Supplementary Files

This is a list of supplementary files associated with this preprint. Click to download.

- SupplementaryInformation.docx
- GraphicalAbstract.jpg